INFLUENCE OF A 3.5 % NaCl SOLUTION ON THE FRACTURE MECHANISMS OF Al- Zn-Mg ALLOYS IN FATIGUE AND TENSION

T. Magnin, P. Rieux, C. Dubessy and J. Le Coze*

This paper analyses and compares the influence of a 3.5 % NaCl solution on the tensile and fatigue properties of a 7020 alloy as a function of the heat treatment and of the electrochemical potential. Stress corrosion cracking and corrosion fatigue occur in very different strain rate ranges at free corrosion potential and the influence of a cathodic potential is not similar in tension and fatigue. The microcracking processes are analysed to explain these differences.

INTRODUCTION

The mechanical properties of high strength aluminium alloys (Al-Cu, Al-Zn-Mg) are very sensitive to the environment and particularly to chloride solutions. The stress corrosion cracking (SCC) behaviour of these alloys has been extensively studied, particularly for the 7000 series alloys in NaCl solutions (1-15). The influence of the heat treatment and of the corresponding microstructure of precipitates on the intergranular cracking in stress corrosion has been clearly established. Nevertheless, the respective influences of the anodic dissolution and the hydrogen embrittlement on the SCC damage are still under discussion. Some authors (1-5, 14) indicate that cracking is controlled by the dissolution (assisted by the mechanical stress) of the intergranular $MgZn_2$ precipitates. The influence of the metallurgical factors such as the size, the coherency and the distribution of the precipitates, the width of the precipitate free zones (PFZ) and the intergranular segregation of Zn and Mg has been analysed and correlated with the dissolution process.

* Département Matériaux, Ecole des Mines, Saint-Etienne (France)

Nevertheless, other studies (6-11) have pointed out the main effect of the hydrogen embrittlement and have also correlated this embrittlement with the influence of the heat treatment and the corresponding microstructure on the SCC resistance. Finally, some authors (11,16) showed that the overall SCC process operates by the combined effect of hydrogen embrittlement and anodic dissolution.

Moreover, if the mechanisms by which an aqueous NaCl solution affects the tensile properties of Al-Zn-Mg alloys are still under controversy, only a few studies have focussed on the influence of Cl^- solutions on the cyclic properties of these alloys (see (17)). Little attention has been paid on the interfacial region between corrosion-fatigue and stress corrosion cracking.

Thus, the aim of this paper is to analyse and compare the influence of the 3.5 % NaCl solution on the tensile and fatigue fracture mechanisms of a weldable 7020 aluminium alloy as a function of the heat treatment and the electrochemical potential.

EXPERIMENTAL

Experiments were performed on a 7020 aluminium alloy the composition of which (in weight %) is : Al-5.1 Zn-1.1 Mg-0.25 Cr-0.15 Si- 0.20 Fe - (< 0.005) Mn - (< 0.005) Cu. Smooth specimens (5 mm diameter, 15 mm gauge length) were machined from rolled plates : the tensile axes were parallel to the rolling direction (for more details of the grain structure, see (18)). They were solution treated at 470°C for 1 hour, then waterquenched.
Two heat treatments (T4 and T6DR) were considered:
(1) T4 corresponds to an ageing at room temperature for 8 days (underageing).
(2) T6DR corresponds to T4 + 24h at 120°C + 24h at 140°C (peak ageing).

During ageing, the precipitation sequence is: GP zones $\rightarrow \eta' \rightarrow \eta$ ($MgZn_2$). The development of the microstructure in the present alloy (18) shows that, for T4, GP zones and η' are present and that for T6DR η' and η precipitates and PFZ can be observed.

SCC tests were performed on smooth specimens using the constant strain rate method (19) in the strain rate range $10^{-8}\ s^{-1} < \dot{\varepsilon} < 10^{-2}\ s^{-1}$. Corrosion-fatigue tests were conducted in tension-compression under symmetrical plastic strain control ($10^{-4} < \pm\Delta\varepsilon_p/2 < 10^{-2}$), at constant strain rate $10^{-5} s^{-1} < \dot{\varepsilon} < 10^{-2} s^{-1}$) using a servo-hydraulic machine (for more technical details, see (20)). Tests were performed in an aerated 3.5 % NaCl solution at pH 6. Very sensitive potentiostatic equipment is used to record during the tests the evolution of the electrochemical parameters. Tests were performed either at free potential ($E=E_o$)

or at imposed cathodic potentials. These potentials are referred to a saturated calomel electrode (SCE). For the 7020 alloys, the free potentials E_o are: E_o(T4) = - 950 mV/SCE and E_o (T6DR) = - 890 mV/SCE. The polarization curves have been published elsewhere (18). The sensitivity to SCC is given by the reduction of the elongation to rupture A in the corrosive solution, compared to dry air. The sensitivity to corrosion fatigue is described in terms of reduction of the number of cycles Ni corresponding to a 1 % decrease of the saturation peak stress (and also to the formation of a 1 mm long crack in the 7020 alloy). Finally, to quantify the evolution of the surface roughness (microcracking) in SCC and in corrosion fatigue, replicas of the specimen surface are taken for different fractions of the specimen lifetimes. They are then analysed using optical and scanning electron microscopy to determine the number of microcracks per unit area.

EXPERIMENTAL RESULTS

Influence of the 3.5 NaCl solution on the tensile properties. Figure 1 shows the influence of the corrosive solution on the tensile properties of the 7020 T6DR alloy at $\dot{\varepsilon} = 2.10^{-7} s^{-1}$ and $E = E_o$. The elongation to fracture A is about 20 % in dry air and decreases to about 5 % in the 3.5 % NaCl solution. The SCC domains of both the 7020 T6DR and 7020 T4 alloys at free corrosion potential E_o are indicated by the curves $A = f(\dot{\varepsilon})$ (fig. 2). It can be noticed that : (i) there is no effect of $\dot{\varepsilon}$ on the value of A in dry air. (ii) The reduction of A in the corrosive solution occurs for $\dot{\varepsilon} < 8.10^{-7} s^{-1}$ for the 7020 T6DR alloy but already for $\dot{\varepsilon} < 2.10^{-5} s^{-1}$ for the 7020 T4 alloy. (iii) At $\dot{\varepsilon} = 2.10^{-7} s^{-1}$, A is reduced by a factor 4 for the 7020 T6DR alloy and by a factor 8 for the 7020 T4 alloy.All these results clearly show a more sensitive effect of the 3.5 % NaCl solution at $E = E_o$ on the 7020 T4 alloy than on the 7020 T6DR alloy.

Characteristic features of the fracture surface of a 7020 T6DR specimen strained at $\dot{\varepsilon} = 2.10^{-7} s^{-1}$ in the corrosive solution are presented on figure 3. An intergranular cracking corresponding to the SCC zone (fig. 3a) and a transgranular ductile cracking corresponding to the final mechanical rupture (fig. 3b) can be observed. To follow the evolution of the SCC damage, the number N_T of cracks per unit area ($1mm^2$) has been determined for different fractions of the plastic elongation (fig. 4) for the 7020 T4 alloy. It is very interesting to notice that cracks initiate at very low plastic strain (0.1 %).

Finally, the influence of a cathodic potential on the tensile properties of the 7020 T6DR alloy has been investigated at an imposed strain rate $\dot{\varepsilon} = 2.10^{-7} s^{-1}$ for which SCC occurs at $E = E_o$. The obtained results at E = - 1100 mV/SCE (fig. 5) clearly show that, contrarily to the observations at $E = E_o$, the elongation to rupture A is not reduced in regard to the behaviour in air.

Influence of the 3.5 % NaCl solution on the cyclic properties

The cyclic evolution of the peak stress σ of the 7020 T6DR alloy in air and in the 3.5 % NaCl solution at $E = E_o$ is presented on the figure 6 for $\dot{\varepsilon} = 2.10^{-3} s^{-1}$ and $\Delta\varepsilon_p/2 = 10^{-3}$. It can be noticed that : (i) σ is identical in air and in the corrosive solution, (ii) the fatigue life is reduced by a factor 4.5 in the corrosive solution. The figure 7 gives the cyclic stress-strain relations $\sigma_s = f(\Delta\varepsilon_p/2)$ of the different alloys. A very pronounced cyclic hardening of the 7020 T4 alloy is observed both in air and in the corrosive solution.

The influence of the imposed strain rate $\dot{\varepsilon}$ on the number of cycles Ni to crack initiation is indicated by the table 1 for the 7020 T4 and T6 DR alloys.

TABLE 1 - Influence of $\dot{\varepsilon}$ on the corrosion fatigue behaviour of 7020 T4 and T6DR alloys, at $(\Delta\varepsilon_p/2) = \pm 10^{-3}$ and $E = E_o$ (Ni (NaCl) = Ni in the 3.5 % NaCl solution))

$\dot{\varepsilon}$ (s^{-1})	2.10^{-3}		2.10^{-4}		4.10^{-5}	
	T4	T6DR	T4	T6DR	T4	T6DR
$\frac{Ni\ (NaCl)}{Ni\ (air)}$	0.3	0.22	0.32	0.35	--	0.40

It can be observed that : (i) Corrosion-fatigue occurs in a strain rate range for which no SCC has been encountered. (ii) The reduction in the fatigue life is very pronounced for both alloys and seems to decrease when $\dot{\varepsilon}$ decreases for the T6DR alloy.

To quantify the fatigue damage evolution, replicas of the specimen surface were taken for different fractions of Ni at $(\Delta\varepsilon_p/2) = \pm 10^{-3}$ and $\dot{\varepsilon} = 2.10^{-3}\ s^{-1}$. The evolution of the total number N_T of cracks per unit area as a function of N/Ni is indicated by the figure 8 for both alloys in air and in the corrosive solution. It clearly appears that : (i) N_T is lower in the corrosive solution than in air. (ii) The number of cracks during corrosion fatigue is one order of magnitude higher than during SCC. (iii) Since transgranular cracking starts at N/Ni = 0.4 in air (i.e. $N \simeq 400$ for the T6DR alloy and $N \simeq 800$ for the alloy), it is obvious that the corrosive solution accelerates the initiation and the micropropagation of cracks both in the T6DR alloy (Ni(NaCl $\simeq$ 220 cycles) and in the T4 alloy (Ni (NaCl) $\simeq$ 650 cycles). Nevertheless, contrarily to the behaviour in SCC

(fig. 4), microcracks do not form during the first cycles.

The observation of the fracture surface after cycling of the 7020 T6DR alloy in the corrosive solution indicates a classical feature of striations (fig. 9).

As for SCC, the influence of an imposed cathodic potential on the corrosion fatigue behaviour of 7020 T6DR specimens has been analysed. At E = - 1100 mV/SCE, $(\Delta\varepsilon_p/2) = \pm 10^{-3}$ and $\dot{\varepsilon} = 2.10^{-3} s^{-1}$, Ni is 680 cycles (± 50). This result shows reduction of the fatigue life (Ni ≃ 1000 cycles in dry air) which is nevertheless lower than the reduction at free corrosive potential $E = E_o$ (Ni ≃ 220 cycles).

DISCUSSION AND CONCLUSIONS

The results presented in this paper clearly show that the influence of a 3.5 % NaCl solution at pH 6 on the tensile and the fatigue properties of the 7020 alloys is very sensitive to the imposed strain rate. SCC and corrosion fatigue occurs for completely different strain rate ranges.

At free potential, SCC occurs at $\dot{\varepsilon} < 2.10^{-5} s^{-1}$ for the 7020 T4 alloy and at $\dot{\varepsilon} < 8.10^{-7} s^{-1}$ for the 7020 T6DR alloy. At $\dot{\varepsilon} = 2.10^{-7} s^{-1}$, the elongation to rupture is reduced by a factor 4 for the T6DR alloy and by a factor 8 for the T4 alloy in comparison to the behaviour in dry air. Corrosion fatigue occurs for both alloys at much higher strain rate than SCC ($\dot{\varepsilon} = 10^{-4}$ to $10^{-2} s^{-1}$). At $\dot{\varepsilon} = 2.10^{-3} s^{-1}$ and $\Delta\varepsilon_p/2 = 10^{-3}$, the fatigue life is reduced by a factor 4 for the T6DR alloy and by a factor 3.5 for the T4 alloy in comparison to the behaviour in air.

At imposed cathodic potential, no SCC damage is observed in the strain rate range for which SCC occurs at free potential. However, a reduction of the fatigue life is observed in the strain rate range for which corrosion fatigue occurs at free potential E_o. Nevertheless, this reduction is lower than those at $E = E_o$.

The analysis of the evolution of the surface damage during fatigue and tension in air and in the 3.5 % NaCl solution is very useful in explaining these observations. Many studies have shown that hydrogen pick-up plays an important role in SCC and also in corrosion fatigue cracking (17) of the 7000 series alloys rather than the anodic dissolution. Nevertheless the localization of the hydrogen reduction reaction is of prior importance to induce embrittlement. During fatigue, microcracks can form at high strain rates well before any change in the saturation stress can be detected. For instance, at $(\Delta\varepsilon_p/2) = \pm 10^{-3}$ in air, microcracks initiate at N/Ni ≃ 0.4 on the T6DR alloy (fig. 8). Thus, during corrosion fatigue, the hydrogen reduction

can be localized at the crack tips and this situation enhances the hydrogen embrittlement. During corrosion fatigue at cathodic potentials, when the microcracks are mechanically formed, hydrogen embrittlement can occur which induces a reduction of the fatigue life. But this evolution is impossible during SCC at the same potentials because no microcracks are mechanically formed in this case. At free corrosion potential, the breakdown of the passive film which occurs both in SCC and in corrosion fatigue enhances the initiation of microcracks. This seems quite obvious for the intergranular stress corrosion microcracking which occurs at low strain rate and low plastic strain amplitude (0.1 % at $\dot{\varepsilon} \simeq 2.10^{-6} s^{-1}$ for the 7020 T4 alloy). During corrosion fatigue at higher strain rates (for which the microcracks are much more numerous than during stress corrosion) the cyclic rupture of the passive film at the emergence of well localized slip bands can accelerate the formation of transgranular fatigue microcracks. In both cases, the hydrogen reduction is then localized at microcrack tips, which induces a localized embrittlement, the micro-propagation of the microcracks and the final rupture.

Even if the same embrittlement mechanisms may be operative in both SCC and corrosion fatigue, this study clearly emphasizes the differences between the two processes. These differences can be correlated with the microcracks formation and evolution which are very different during fatigue and tension in the 3.5 % NaCl solution. This explains why SCC and corrosion fatigue can occur in completely different strain rate ranges.

REFERENCES

(1) Sedriks, A.J., Slattery, P.W. and Pugh, E.N., Trans. ASM, 62, 1969, p. 238.

(2) Sedricks, A.J., Green, J.A.S. and Novak, D.L., Met. Trans., 1, 1970, p. 1815.

(3) Taylor, I.T. and Edgar, R.L., Met. Trans., 2, 1971, p. 833.

(4) Doig, P. and Edington, J.W., Met. Trans., A, 6A, 1975, p. 943

(5) Doig, P. and Edington, J.W., Corrosion, 31, 10, 1975, p. 347.

(6) Montgrain, L. and Swann, P.R., "Hydrogen in Metals", Edited by I. Bernstein and A. Thompson, ASM, 1974, p. 575.

(7) Speidel, M.O., ibid, 1974, p. 249.

(8) Gest, R.J. and Troiano, A.R., Corrosion, 30, 1974, p. 274.

(9) Scamans, G.M., Alani, R. and Swann, P.R., Corros. Sci., 16, 1976, p. 443.

(10) Hardie, D., Holroyd, N.J. and Parkins, R.N., Met. Sci., 13, 1979, p. 603.

(11) Holroyd, N.J.H. and Hardie, D., Corros. Sci., 21, 1981, p. 129.

(12) Buhl, H., "Stress Corrosion Cracking - The slow strain rate technique", ASTM STP 665, 1976, p. 333.

(13) Green, J.A.S. and Montague, W.G., "Corrosion 77", San Francisco, Edited by NACE, 1977, p. 17.

(14) Choi, Y., Kim, H.L. and Pyun, S.I., Jr. Mat. Sci., 19, 1984, p. 1517.

(15) Sarkar, B., Marck, M. and E.A. Starke, Met. Trans. A, 12A, 1981, p. 1939.

(16) Thompson, A.W., Mater. Sci. Eng., 43, 1980, p. 41.

(17) Holroyd, N.J.H. and Hardie, D., "Environment-Sensitive Fracture", ASTM STP 821, Edited by Ugiansky and Pugh, 1984, p. 534.

(18) Magnin, T. and Dubessy, C., Mem. Et. Sci. Rev. Met., 10, 1984, p. 559.

(19) Parkins, R.N., Br. Corr. Jr., 7, 1972, p. 154.

(20) Magnin, T. and Coudreuse, L., Mat. Sci. Eng., 72, 1985, p. 125.

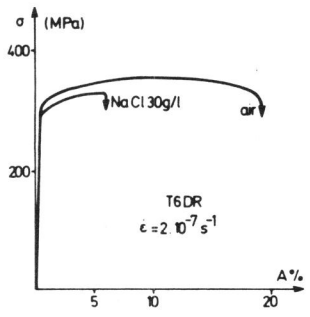

Figure 1 Influence of the 3.5 % NaCl solution on the tensile properties of the 7020 T6DR alloy at $\dot{\varepsilon} = 2.10^{-7}s^{-1}$.

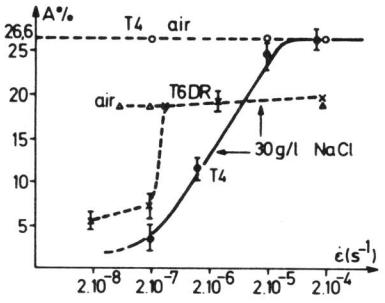

Figure 2 Influence of the heat treatment on the SCC domains of the 7020 alloy.

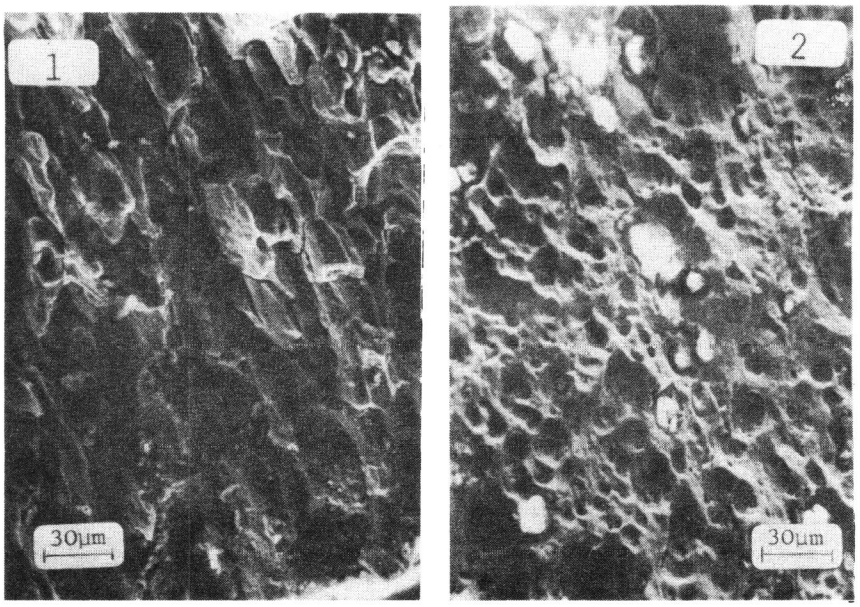

Figure 3 Surface of fracture during SCC of a 7020 T6DR alloy at $\dot{\varepsilon} = 2.10^{-7}s^{-1}$; (1) SCC domain (2) mechanical fracture.

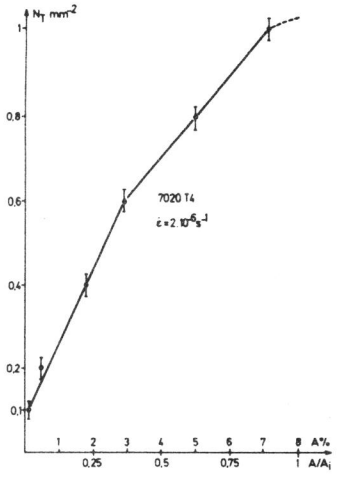

Figure 4 Number of cracks N_T during SCC of a 7020 T4 alloy at $\dot{\varepsilon} = 2.10^{-6}s^{-1}$.

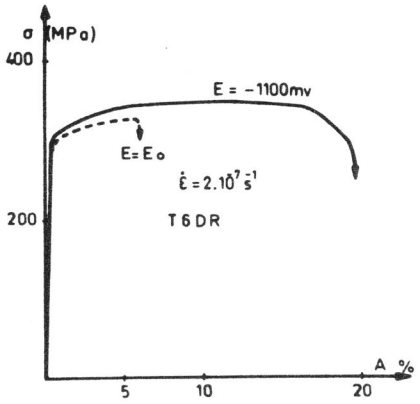

Figure 5 Influence of a cathodic potential on the tensile properties of a 7020 T6DR alloy at $\dot{\varepsilon} = 2.10^{-7}s^{-1}$.

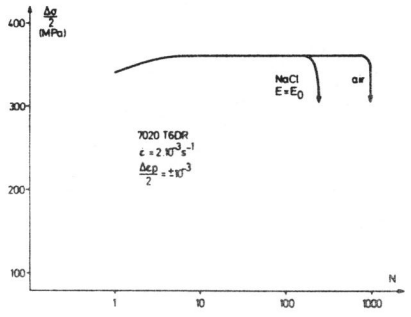

Figure 6 Evolution of the peak stress σ during fatigue of a 7020 T6DR alloy at $\Delta\varepsilon_p/2 = 10^{-3}$ and $\dot{\varepsilon} = 2.10^{-3}s^{-1}$.

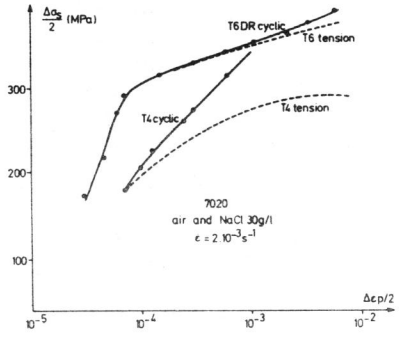

Figure 7 Cyclic stress-strain curves of the 7020 alloy at $\dot{\varepsilon} = 2.10^{-3}s^{-1}$.

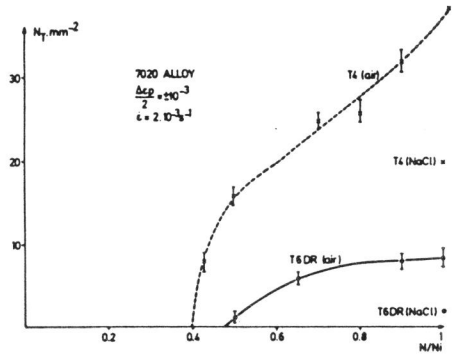

Figure 8 Evolution of the number of cracks N_T during fatigue of a 7020 alloy in air and at N = Ni in the corrosive solution.

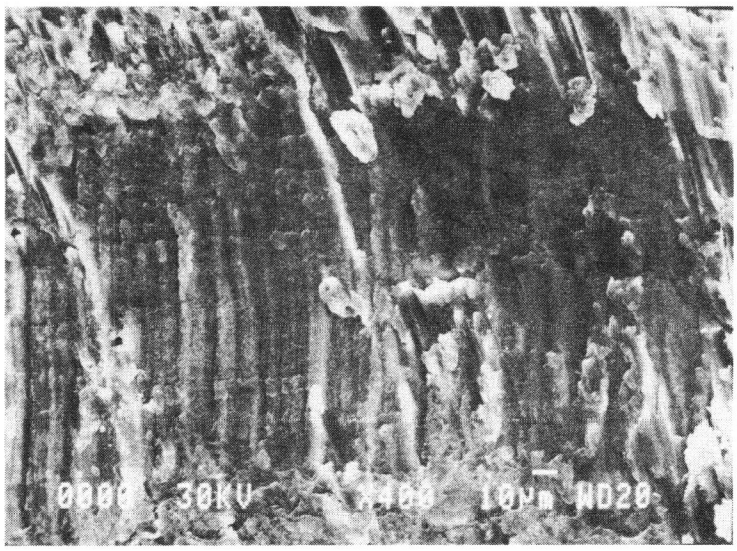

Figure 9 Surface of fracture after corrosion fatigue (7020 T6DR alloy at $\Delta\varepsilon_p/2 = 10^{-3}$ and $\dot{\varepsilon} = 2.10^{-3}s^{-1}$).